Atmos. Chem. Phys. Discuss., 10, 14611–14637, 2010
www.atmos-chem-phys-discuss.net/10/14611/2010/
doi:10.5194/acpd-10-14611-2010

Atmospheric Chemistry and Physics Discussions

Variation of particle number size distributions and chemical compositions at the urban and downwind regional sites in the Pearl River Delta during summertime pollution episodes

D. L. Yue[1], M. Hu[1], Z. J. Wu[1,2], S. Guo[1], M. T. Wen[1], A. Nowak[2], B. Wehner[2], A. Wiedensohler[2], N. Takegawa[3], Y. Kondo[3], X. S. Wang[1], Y. P. Li[1], L. M. Zeng[1], and Y. H. Zhang[1]

[1]State Key Joint Laboratory of Environmental Simulation and Pollution Control, College of Environmental Sciences and Engineering, Peking University, Beijing, 100871, China
[2]Leibniz Institute for Tropospheric Research, Permoserstrasse 15, 04318 Leipzig, Germany

[3] Research Center for Advanced Science and Technology, University of Tokyo, Tokyo 153-8904, Japan

Received: 8 March 2010 – Accepted: 2 June 2010 – Published: 11 June 2010

Correspondence to: M. Hu (minhu@pku.edu.cn)

Published by Copernicus Publications on behalf of the European Geosciences Union.

ACPD
10, 14611–14637, 2010

Abstract

In order to characterize the features of particulate pollution in the Pearl River Delta (PRD) in the summer, continuous measurements of particle number size distributions and chemical compositions were simultaneously performed at Guangzhou urban site (GZ) and Back-garden downwind regional site (BG) in July 2006. Particle number concentration from 20 nm to 10 µm at BG was $(1.7\pm0.8)\times10^4$ cm^{-3}, about 40% lower than that at GZ, $(2.9\pm1.1)\times10^4$ cm^{-3} with intensive traffic emissions. The total particle volume concentration at BG was 94 ± 34 µm^3 cm^{-3}, similar to that at GZ, 96 ± 43 µm^3 cm^{-3}. More 20–100 nm particles, significantly affected by the traffic emissions, were observed at GZ, while 100–660 nm particle number concentrations were similar at both sites as they are more regional. $PM_{2.5}$ values were also similar at GZ (69 ± 43 µg m^{-3}) and BG (69 ± 58 µg m^{-3}), indicating the fine particulate pollution in the PRD region to be regional. Two kinds of pollution episodes, the accumulation pollution episode and the regional transport pollution episode, were observed. Fine particles over 100 nm dominated both number and volume concentrations of total particles during the late periods of these pollution episodes. Accumulation and secondary transformations are two main reasons for the nighttime accumulation pollution episode. SO_4^{2-}, NO_3^-, and NH_4^+ accounted for about 60% in 100–660 nm particle mass and $PM_{2.5}$. When south or south-southeast wind prevailed in the PRD region, regional transport of pollutants takes place. Regional transport contributed about 30% to fine particulate pollution at BG during a regional transport case. Secondary transformation played an important role during regional transport, causing higher increase rates of secondary ions in $PM_{1.0}$ than other species and shifting the peaks of sulfate and ammonium mass size distributions to larger sizes. SO_4^{2-}, NO_3^-, and NH_4^+ accounted for about 70% and 40% of $PM_{1.0}$ and $PM_{2.5}$, respectively.

ACPD
10, 14611–14637, 2010

1 Introduction

Atmospheric aerosols have attached more and more attention in recent years because they influence the global climate change and human health (Dockery et al., 1994), and degrade visibility (Sokolik and Toon, 1996; Jung and Kim, 2006). In order to understand these effects, accurate knowledge on physical and chemical properties of aerosol is required. A large number of studies showed that the size resolved properties of the atmospheric aerosols are more powerful to explain their atmospheric behavior than their bulk properties (Dusek et al., 2006; See et al., 2006).

On one hand, the absorbing and scattering effect of aerosols on the incoming radiation is dependent on the particle size and composition (Nishita et al., 2007) and the accumulation mode particle number concentrations could explain the visibility degradation on hazy days (See et al., 2006). On the other hand, only particles within a certain size range have cloud-nucleating ability and affect the microphysical and optical properties of cloud condensation nuclei (CCN, Iorga and Stefan, 2005). In addition, whether the adverse health effects of aerosols are number- or mass-concentration-dependent is still a debating issue. Recently, studies have proved that ultrafine particles with very small sizes can be uptaken directly by cells as well as be translocated to other sensitive target organs such as the heart and central nervous system (Oberdörster et al., 2005). Compared with larger particles of similar composition, ultrafine particles are more toxic and induce more intense oxidative stress in cells (Nel, 2005; Nel et al., 2006). The chemical compositions are also key elements deciding the health effect as well as the influence on climate change. Therefore, characterizing number size distributions and chemical compositions of atmospheric aerosols is very important to understand their effects on climate change, human health, and air quality.

The Pearl River Delta (PRD) is one of the most economically invigorating and densely populated regions and one of the biggest city clusters in the world. Rapid urbanization and economic development have deteriorated the air quality and changed the properties of the air pollution: The primary pollutants, such as SO_2 and inhalable

ACPD
10, 14611–14637, 2010

particulate matter (PM_{10}) have been reduced by abatement measures. However, the secondary products such as ozone and fine particles of high concentrations become the main issues especially in the summer. They have gained widespread public concerns in recent years as both have a large impact on human health and regional air quality as well as global climate at high concentrations. Moreover, the scale of the problems in the PRD region has also expanded (Zhang et al., 2008). The particle pollution in the PRD region have been reported regarding to the chemical compositions in size resolved particles or in $PM_{2.5}$ and PM_{10} at one or more sites and particle number size distributions at a coastal rural site Xinken (Cao et al., 2004; Hagler et al., 2006; Liu et al., 2008a, b; Zhang et al., 2008). However, simultaneous measurements of particle number size distributions and chemical compositions at over one site in the PRD region have not been reported.

Within the "Program of Regional Integrated Experiments of Air Quality over the Pearl River Delta" intensive campaign in July 2006 (PRIDE-PRD2006) focusing on gas phase photochemistry and the aerosol formation and properties during summertime, the particle number size distributions were measured simultaneously at both Guangzhou (GZ) urban site and Back-garden (BG) downwind regional site, as well as the concentrations of mass and chemical composition of fine particles. Previous papers in the same special issue already show that the conditions were mainly characterized by strong particulate pollution at ground level (Li et al., 2010) and size mattered more than chemistry for the CCN activity of aerosol particles at the BG site in the summer of 2006 (Rose et al., 2010). Hence, the purpose of this study is to characterize the particulate pollution in the PRD region on the basis of comparison of particle number size distributions and chemical compositions between the two sites and to explore secondary formation and regional transport with the discussion of pollution episodes.

ACPD
10, 14611–14637, 2010

2 Experimental methods

The intensive field campaign was performed simultaneously at both GZ and BG sites in July 2006 (Zhang et al., 2010). At the GZ site the instruments were set up on the top floor of Guangdong Provincial Environmental Protection Monitoring Center (about 50 m a.g.l.), which is located in the western urban area of Guangzhou city. At the BG site the instruments were installed on the roof of a hotel building (about 15 m a.g.l.), which is located in the north of Huadu district, about 50 km north from the GZ site.

At the GZ site dry particle number size distributions between 15 nm and 10 µm were measured with a system consisting of a Scanning Mobility Particle Sizer (SMPS, TSI model 3080, TSI Inc., St. Paul, MN, USA) and an Aerodynamic Particle Sizer (APS, TSI model 3321). The SMPS (a long differential mobility analyzer (TSI model 3081) with a Condensational Particle Sizer (CPC, TSI model 3025A)) was used to measure particle number size distributions from 15 to 660 nm with a time resolution of 5 min. The system was kept dry by silica gel tube within the inlet line.

At the BG site the particle number size distributions from 3 nm to 10 µm were measured with a system consisting of a Twin Differential Mobility Particle Sizer (TDMPS) and an APS (TSI model 3321, USA). The TDMPS is composed of two Hauke-type differential mobility analyzers and two CPCs (TSI model 3010 and 3025, respectively, USA), deployed to measure the particle number size distributions from 3 to 900 nm every 10 min. The relative humidity within the whole system was kept below 30% by silica gel tubes within the inlet line and both sheath air cycles.

The size range of particle number size distributions observed by APSs was 500 nm–10 µm. The time resolution of APS was set as 5 or 10 min according to SMPS's or TDMPS's to keep consistent. APS data of particle number size distributions between 660 or 900 nm and 10 µm were transformed from aerodynamic diameter to Stokes diameter with a supposed particle density of 1.7 g cm^{-3} (Yue et al., 2009).

Size-dependent losses due to diffusion and sedimentation within the inlet lines were corrected with empirical particle loss corrections for both two systems (Willeke and

ACPD
10, 14611–14637, 2010

Baron, 1993). The information on these instruments and the time periods of valid data is listed in Table 1.

Other data including $PM_{2.5}$ and mass concentrations of water soluble ions (SO_4^{2-}, NO_3^-, NH_4^+, and Cl^-) and organic matter (OM) in $PM_{1.0}$ or $PM_{2.5}$, meteorological factors (temperature, relatively humidity, wind speed, and wind direction (T, RH, WS, and WD, respectively)), and gaseous pollutants (CO, SO_2, and O_3) at both sites are also involved in this paper. $PM_{2.5}$ was measured by a Tapered Element Oscillating Microbalances (TEOM), ions in $PM_{2.5}$ by two coupled Wet Annular Denuder sampling/Ion Chromatograph analysis systems (WAD/IC), size-resolved chemical composition mass concentrations by Micro Orifice Uniform Deposit Impactor (MOUDI), and CO, SO_2, and O_3 by CO Analyzer, SO_2 Analyzer, and O_3 Analyzer (model 9830A, 9850A, and 9810A, ECOTECH, Australia), respectively. Meteorological stations (Met. Station) were also set up at both sites. In addition, ions and OM in $PM_{1.0}$ were detected by an Aerodyne Mass Spectrometer (AMS) at the BG site. Relevant information is also listed in Table 1.

3 Results and discussion

3.1 Overview of particle number size distributions and mass concentrations

Weather system during summertime in the PRD region is controlled by tropical cyclones and subtropical high pressure alternately. The former brings frequent precipitation and scavenge the pollutants, while the latter leads to high atmospheric stability with high temperature and RH, causing regional pollution. The temperatures during PRIDE-PRD 2006 at both sites were similar, 31±3 °C at GZ and 30±3 °C at BG. RH were identical at GZ and BG, 76±14%. Low wind speeds (below 2 m s^{-1}) were observed during about 60% of the measurement time in the PRD region. Over 50% of the time during PRIDE-PRD 2006 at GZ and BG the wind came from south or southeast.

The mean particle number size and volume distributions at both sites during the

ACPD
10, 14611–14637, 2010

whole campaign are shown in Fig. 1. The ultrafine particle number concentration at the GZ site was significantly higher than that at the BG site. During the measurement period, the particle number concentration (20 nm–10 μm) at GZ t ($(2.9\pm1.1)\times10^4$ cm^{-3}) is 70% higher than that at BG site, $(1.7\pm0.8)\times10^4$ cm^{-3} (Table 2). The explanation is there are more intensive traffic emission sources in the Guangzhou urban area than those in the Back-garden suburban area. The number concentrations at GZ were also significantly higher than the total particle number concentrations (3 nm–10 μm) at Xinken rural coastal site in the PRD region in October of 2004, $(1.6\pm0.8)\times10^4$ cm^{-3} (Liu et al., 2008), which were comparable to the total particle number concentrations at BG, $(1.8\pm0.8)\times10^4$ cm^{-3}.

At both sites fine particles (D_p<1000 nm) were the main contributor to the total particle volume concentrations, as shown in the lower panel of Fig. 1. In the fine particle size range, the particle volume size distributions were similar and no significant difference within the ultrafine sizes was observed at the GZ and BG sites. In coarse mode, the peak of particle volume size distribution at the BG site show at about 2 μm, smaller than that at the GZ site at about 3 μm. This indicates that the major sources for the coarse particles are different at the BG and GZ sites. The total particle volume concentration at the GZ site of 96±43 μm^3 cm^{-3} is similar to that at the BG site (94±34 μm^3 cm^{-3}). In additions, the measured mean particle $PM_{2.5}$ mass concentration is also quite similar at both sites (69±43 μg m^{-3} at GZ and 69±58 μg m^{-3} at BG). These findings suggest that the fine particulate pollution in the PRD region is a regional problem. The higher fine particle mass concentrations and total particle volume concentrations at the GZ and BG sites than those at Xinken, 60 km southeast of Guangzhou with a rural/coastal background character, is probably caused by the influence of the sea breeze at Xinken (Zhang et al., 2008).

ACPD
10, 14611–14637, 2010

3.2 Characteristics of pollution episodes

According to the frequency distribution of hourly averaged $PM_{2.5}$, time periods with $PM_{2.5}$ exceeding 100 $\mu g\,m^{-3}$ (90% of time $PM_{2.5}$ is below 100 $\mu g\,m^{-3}$) for more than two hours (excluding those caused by short time local emissions) at both sites were classified as pollution episodes in this paper. Totally, pollution episodes were observed on five days (12, 14, 19, 21, 23 July) from 6 to 23 July. Mainly two different kinds of pollution episodes were identified, accumulation pollution episode (cases on 12, 14, and 23 July) and regional transport pollution episode (cases on 19 and 21 July).

3.2.1 Accumulation pollution episode

Pollution episodes with gradual increase of $PM_{2.5}$ mass concentrations were observed at both sites simultaneously. Such pollution episodes took place under stagnant meteorological conditions with wind speed below 1 $m\,s^{-1}$, RH over 80%, and low boundary layer at night.

One accumulation pollution episode occurred from about 18:00 LT on 11 July to about 06:00 LT on 12 July is illustrated in Figs. 2 and 3 (Accumulation pollution episodes on 14 and 23 July will not be discussed in detail in this paper as they were not observed completely.). During this episode, a clear particle growth process was observed: The number peak diameter at about 80 nm in the beginning grew gradually to at about 120 nm in 12 h (Fig. 4). The evident increase in particle number concentration from 100 to 660 nm was observed. Conversely, the number concentrations for particles from 3 to 20 nm and from 20 to 100 nm decreased during the episode. In the early morning of 12 July, the lowest number concentration of the 3–20 nm particles occurred (around 10 cm^{-3}). This can be ascribed to the strong coagulation scavenging produced by the high concentration of the accumulation mode particles (Mönkkönen et al., 2004).

The obvious increases of $PM_{2.5}$ and secondary ions in $PM_{2.5}$ including SO_4^{2-} and NO_3^- were also observed at both sites, as shown in Fig. 3. Two main reasons for this increase can be postulated: (1) The dispersion of primary emissions was very weak

ACPD
10, 14611–14637, 2010

under stable weather conditions. It was confirmed by the fact that CO and EC kept increasing gradually during this episode. (2) Secondary transformation processes play a key role in the particle growth. Evident growth in secondary water-soluble ions mass concentrations was observed.

During this episode, the increase rates of $N_{100-660}$ and $V_{100-660}$ were about 400 $cm^{-3}\,h^{-1}$ and 4.0 $\mu m^3\,m^{-3}\,h^{-1}$, respectively (Table 3). If the average density of 100–660 nm particles is assumed to be 1.43 $g\,cm^{-3}$ as estimated in the summer of Beijing (Yue et al., 2009), the latter was equal to 5.7 $\mu g\,m^{-3}\,h^{-1}$. The increase rates of SO_4^{2-} and NO_3^- in $PM_{2.5}$ were 2.4 and 0.6 $\mu g\,m^{-3}\,h^{-1}$, respectively. SO_4^{2-} increased significantly faster than NO_3^-, partly because of the lower volatility of SO_4^{2-}. The sum concentration of SO_4^{2-}, NO_3^-, and NH_4^+ accounted for about 60% in $PM_{2.5}$, if the measured SO_4^{2-} and NO_3^- are neutralized by NH_4^+. Almost all SO_4^{2-}, NO_3^-, and NH_4^+ are in the form of fine particles, and most SO_4^{2-}, NO_3^-, and NH_4^+ are in 100–660 nm particles. If we assume that 80% of SO_4^{2-} and NO_3^- in $PM_{2.5}$ are in 100–660 nm particles according to the measured average chemical composition size distributions by MOUDI and the measured SO_4^{2-} and NO_3^- are neutralized by NH_4^+, SO_4^{2-}, NO_3^-, and NH_4^+ (actually 80% of the sum concentration of SO_4^{2-}, NO_3^-, and NH_4^+ in $PM_{2.5}$) can explain about 60% of the 100–660 nm particle mass increase. During the same period, the corresponding increase ratios of some species at the GZ site were also given in Table 3. The corresponding increase rates at the GZ site were usually higher than those at BG site. The possible reasons might be that the percentage of SO_4^{2-}, NO_3^-, and NH_4^+ was larger in $PM_{2.5}$ at the urban site GZ (about 40%) than at the regional site BG (about 25%), so particles grow more under the condition with high RH during nighttime at GZ. It is consistent with the fact that increase rates at Peking University, an urban site in Beijing are higher than those at Yufa, a regional site in Beijing, during accumulation pollution episodes (Yue et al., 2009).

ACPD
10, 14611–14637, 2010

3.2.2 Regional transport pollution episode

On 19 and 21 July the number concentrations of particles within 100–660 nm, mass concentrations of SO_4^{2-}, and mixing ratios of NO_2 at BG showed peaks 6 to 8 h behind corresponding peaks appeared at GZ in the afternoon (Fig. 5. With the average wind speed of 2 m s^{-1}, it takes about 7 h to transport from GZ to BG). It was observed with south or southeast wind prevailing at both sites (Figs. 5 and 6b), indicating air masses move from south or south east. These findings suggest that when south or south east wind prevails in the PRD region, regional transport of pollutants including particles takes place. In the afternoon of 19 and 21 July, particles around 100 nm at GZ decreased gradually, but particles around 100 nm at BG increased quickly at the same time, shifting the geometric mean diameter of these particles at BG to larger sizes (Fig. 7a). The average mass size distribution of SO_4^{2-} and NH_4^+ on 21 July also peaked at larger sizes at BG (Fig. 7b). The average equivalent ratio of sulfate to total sulfur ($SO_4^{2-}/(SO_4^{2-}+SO_2)$) at BG was 0.4±0.1, about 30% higher than that at GZ, 0.3±0.1. In addition, the mass size distribution of oxalate peaked at a larger size with higher peak value at BG compared with GZ. These results suggest that during such a transport process, particles became to be aged. The contribution of secondary formed fraction to fine particles increased significantly.

Compared with on 19 and 21 July, there were similar wind speeds (below 3 m s^{-1}) but different wind directions from the west or northwest to the BG site (Fig. 7a) on 12 and 13 July, where lay the mountains. So when the wind comes from this direction, it brings clean air, and 12 and 13 July were taken as the contrast days without obvious regional pollutant transport. In order to quantify the contribution of regional transport to the fine particulate pollution at BG, average particle number and volume concentrations from 100 to 660 nm, $PM_{2.5}$, and mass concentrations of the chemical compositions in $PM_{1.0}$, including secondary ions (SO_4^{2-}, NO_3^-, and NH_4^+) and OM during the time period from 12:00 LT to 24:00 LT on 12 and 13 July without obvious regional transport and on 19 and 21 July with regional transport are compared in Table 4. They all increased

ACPD
10, 14611–14637, 2010

significantly with regional transport. The contribution of regional transport to $N_{100-660}$ was around 35%. The contribution of regional transport of $V_{100-660}$ was similar to that of $PM_{2.5}$, close to 30%. The higher increase rates of secondary ions in $PM_{1.0}$ (38% on average) than that of OM (23%) indicated that during the transport secondary transformation occurred and deteriorated the particulate pollution. SO_4^{2-}, NO_3^-, and NH_4^+ accounted for about 70% of $PM_{1.0}$ ($PM_{1.0}$=SO_4^{2-}+NO_3^-+NH_4^++OM) and about 40% of $PM_{2.5}$, suggesting that SO_4^{2-}, NO_3^-, and NH_4^+ are the major composition of fine particles and play a very important role in the regional transport pollution episode.

4 Summary and conclusions

Particle number concentration from 20 nm to 10 µm in the summer of 2006 at the GZ site was 70% higher than that at the BG site. Resulted from intensive traffic emissions, more 20–100 nm particles were observed at GZ, while 100–660 nm particle number concentrations were similar at both sites as they are more regional. The total particle volume concentrations and $PM_{2.5}$ were similar at the GZ site (96±43 $\mu m^3\,cm^{-3}$, 69±43 $\mu g\,m^{-3}$) and BG site (94±34 $\mu m^3\,cm^{-3}$, 69±58 $\mu g\,m^{-3}$), indicating that particulate pollution in the PRD region is a regional problem.

Two kinds of pollution episodes, the accumulation pollution episode and the regional transport pollution episode, were observed. Fine particles over 100 nm dominated both number and volume concentrations of total particles during the late periods of these pollution episodes. Accumulation and secondary transformations are two main reasons for the nighttime accumulation pollution episode, with the increase rates of SO_4^{2-} and NO_3^- to be 2.4 and 0.6 $\mu g\,m^{-3}\,h^{-1}$, respectively. SO_4^{2-}, NO_3^-, and NH_4^+ account for about 60% in 100–660 nm particle mass and $PM_{2.5}$. When south or south east wind prevailed in the PRD region, regional transport of pollutants takes place. The contribution of regional transport was about 30% to fine particulate pollution at the BG site during a regional transport case. Secondary transformation occurred and played an

ACPD
10, 14611–14637, 2010

important role during regional transport, causing higher increasing rates of secondary ions (including SO_4^{2-}, NO_3^-, and NH_4^+) in $PM_{1.0}$ than other species and shifting the peaks of sulfate, ammonium, and oxalate mass size distributions to larger sizes. SO_4^{2-}, NO_3^-, and NH_4^+ accounted for about 70% in $PM_{1.0}$ and about 40% in $PM_{2.5}$.

Pollution episodes in the PRD region during summertime are usually contributed by secondary transformation, causing the main contributor of total particle number concentration as well as volume concentration to be fine particles over 100 nm with major composition of SO_4^{2-}, NO_3^-, and NH_4^+. Hence, these particles will dominate CCN and impose significant effect on visibility degradation during the pollution episodes in the PRD region. Control of the precursors of SO_4^{2-}, NO_3^-, and NH_4^+ will effectively help to reduce the fine particulate pollution and decrease the influence of the aerosols in the PRD region during the summertime.

Acknowledgements. This research was supported by the National High-tech R&D Program (863 Program, 2006AA06A308) and the National Basic Research Program (2002CB211605, 2002CB410801) from Ministry of Science & Technology, China. The author would also like to thank Fan Yang, Rui Xiao, Weiwei Hu, Jianwei Gu, and Hang Su for supplying important data for this paper.

References

Barsanti, K. C., McMurry, P. H., and Smith, J. N.: The potential contribution of organic salts to new particle growth, Atmos. Chem. Phys., 9, 2949–2957, doi:10.5194/acp-9-2949-2009, 2009.

Bond, T. C., Wehner, B., Plewka, A., Wiedensohler, A., Heintzenberg, J., and Charlson, R. J.: Climate-relevant properties of primary particulate emissions from oil and natural gas combustion, Atmos. Environ., 40(19), 3574–3587, 2006.

Cao, J. J., Lee, S. C., Ho, K. F., Zou, S. C., Fung, K., Li, Y., Watson, J. G., and Chow, J. C.: Spatial and seasonal variations of atmospheric organic carbon and elemental carbon in Pearl River Delta Region, China, Atmos. Environ., 38, 4447–4456, 2004.

ACPD
10, 14611–14637, 2010

Dockery, D. W. and Pope, C. A.: Acute respiratory effects of particulate air pollution, Annu. Rev. Publ. Health, 15, 107–132, 1994.
Dusek, U., Frank, G. P., Hildebrandt, L., et al.: Size matters more than chemistry for cloud-nucleating ability of aerosol particles, Science, 312, 1375–1378, 2006.
Hagler, G. S. W., Bergin, M. H., Salmon, L. G. et al.: Source areas and chemical composition of fine particulate matter in the Pearl River Delta region of China, Atmos. Environ., 40, 3802–3815, 2006.
Hu, M., Wu, Z.J., Slanina, J., et al.: Acidic gases, ammonia and water-soluble ions in $PM_{2.5}$ at a coastal site in the Pearl River Delta, China, Atmos. Environ., 42, 6310–6320, 2008.
Iorga, G. and Stefan, S.: Effects of the atmospheric aerosol on the optical properties of cloud, Rom. Rep. Phys., 57(3), 426–435, 2005.
Jung, C. H. and Kim, Y. P.: Numerical estimation of the effects of condensation and coagulation on visibility using the moment method, J. Aerosol Sci., 37(2), 143–161, 2006.
Li, X., Brauers, T., Shao, M., Garland, R. M., Wagner, T., Deutschmann, T., and Wahner, A.: MAX-DOAS measurements in southern China: retrieval of aerosol extinctions and validation using ground-based in-situ data, Atmos. Chem. Phys., 10, 2079–2089, doi:10.5194/acp-10-2079-2010, 2010.
Liu, S., Hu, M., Slanina, S., He, L. Y., Niu, Y. W., Bruegemann, E., Gnauk, T., and Herrmann, H.: Size distribution and source analysis of ionic compositions of aerosols in polluted periods at Xinken in Pearl River Delta (PRD) of China, Atmos. Environ., 42, 6284–6295, 2008a.
Liu, S., Hu, M., Wu, Z. J., Wehner, B., Wiedensohler, A., and Cheng, Y. F.: Aerosol number size distribution and new particle formation at a rural/coastal site in Pearl River Delta (PRD) of China, Atmos. Environ., 42, 6275–6283, 2008b.
Mozurkewich, M.: The dissociation constant of ammonium nitrate and its dependence on temperature, relative humidity and particle size, Atmos. Environ., 27A(2), 261–270, 1993.
Mönkkönen, P., Koponen, I. K., Lehtinen, K. E. J. et al.: Death of nucleation and Aitken mode particles: observations at extreme atmospheric conditions and their theoretical explanation, J. Aerosol Sci., 35(6), 781–787, 2004.
Nel, A.: Air pollution-related illness: effect of particles, Science, 308, 804–806, 2005.
Nel, A., Xia, T., Madler, L., and Li, N.: Toxic potential of materials at the nanolevel, Science, 311, 622–627, 2006.
Nishita, C., Osada, K., Matsunaga, K., and Iwasaka, Y.: Number-size distributions of free tropospheric aerosol particles at Mt. Norikura, Japan: effects of precipitation and air-mass trans-

ACPD
10, 14611–14637, 2010

portation pathways, J. Geophys. Res., 112, D10213, doi:10.1029/2006JD007969, 2007.
Oberdörster, G., Oberdörster, E., and Oberdörster, J.: An emerging discipline evolving from studies of ultrafine particles, Environ. Health Persp., 113 (7), 823–839, 2005.
Rose, D., Nowak, A., Achtert, P., Wiedensohler, A., Hu, M., Shao, M., Zhang, Y., Andreae, M. O., and Pöschl, U.: Cloud condensation nuclei in polluted air and biomass burning smoke near the mega-city Guangzhou, China – Part 1: Size-resolved measurements and implications for the modeling of aerosol particle hygroscopicity and CCN activity, Atmos. Chem. Phys., 10, 3365–3383, doi:10.5194/acp-10-3365-2010, 2010.
See, S. W., Balasubramanian, R., and Wang, W.: A study of the physical, chemical, and optical properties of ambient aerosol particles in Southeast Asia during hazy and nonhazy days, J. Geophys. Res., 111, D10S08, doi:10.1029/2005JD0061, 2006.
Sokolik, I. N. and Toon, O. B.: Direct radiative forcing by anthropogenic airborne mineral aerosols, Nature, 381(6584), 681–683, 1996.
Takegawa, N., Miyakawa, T., Watanabe, M., Kondo, Y., Miyazaki, Y., Han, S., Zhao, Y., Pinxteren, D., van Bruggemann, E., Gnauk, T., Herrmann, H., Xiao, R., Deng, Z., Hu, M., Zhu, T., Zhang, Y.: Performance of an aerodyne aerosol mass spectrometer (AMS) during intensive campaigns in China in the summer of 2006, Aerosol Sci. Tech., 43, 189–204, 2009.
Wei, F., Teng, E., Wu, G., Hu, W., Wilson, W. E., Chanpman, R. S., Pau, J. C., and Zhang, J.: Ambient concentrations and elemental compositions of PM_{10} and $PM_{2.5}$ in four Chinese cities, Environ. Sci. Technol., 33, 4188–4193, 1999.
Xiao, R., Takegawa, N., Kondo, Y., Miyazaki, Y., Miyakawa, T., Hu, M., Shao, M., Zeng, L. M., Hofzumahaus, A., Holland, F., Lu, K., Sugimoto, N., Zhao, Y., and Zhang, Y. H.: Formation of submicron sulfate and organic aerosols in the outflow from the urban region of the Pearl River Delta in China, Atmos. Environ., 43, 3754–3763, 2009.
Yue, D. L., Hu, M., Wu, Z. J., Wang, Z. B., Guo, S., Wehner, B., Nowak, A., Achtert, P., Wiedensohler, A., Jung, J., Kim, Y. J., and Liu, S. C.: Characteristics of aerosol size distributions and new particle formation in the summer of Beijing, J. Geophys. Res., 114, D00G12, doi:10.1029/2008JD010894, 2009.
Zhang, Y. H., Hu, M., Zhong, L. J., Wiedensohler, A., Liu, S. C., Andreae, M. O., Wang, W., and Fan, S. J.: Regional Integrated Experiments on Air Quality over Pearl River Delta 2004 (PRIDE-PRD2004): overview, Atmos. Environ., 42, 6157–6173, 2008.
Zhang, Y. H., Hu, M., Shao, M., Brauers, T., Chang, C. C., Hofzumahaus, A., Holland, F., Li, X., Lu, K., Kita, K., Kondo, Y., Nowak, A., Pöschl, U. and Rohrer, F., Zeng, L., Wiedensohler, A.,

ACPD
10, 14611–14637, 2010

and Wahner, A.: Continuous efforts to investigate regional air pollution in the Pearl River Delta, China: PRIDEPRD2006 campaign, Atmos. Chem. Phys. Discuss., in preparation, 2010.

ACPD
10, 14611–14637, 2010

Table 1. Measurement of particle number size distributions and other parameters at GZ and BG.

Site	Instrument	Data	Time resolution	Manufacturer	Valid data in Jul	Institute/ Reference
GZ	SMPS	15–660 nm PNSD	5 min	TSI, USA	6–10, 15–30	This paper
	APS	660–10 000 nm PNSD	5 min	TSI, USA	6–10, 23–30	
BG	TDMPS	3–900 nm PNSD	10 min	IfT, Germany	4–14, 16–23	This paper
	APS	900–10 000 nm PNSD	10 min	TSI, USA		
GZ&BG	TEOM	$PM_{2.5}$	1 min	Thermo, USA	Used when necessary and available	PKU
	WAD/IC	Ions in $PM_{2.5}$	30 min	PKU, China		
	MOUDI	Size resolved ions in PM_{18}	about 12 h	MSP, USA		
	Met. Station	T, RH, WS, WD	10 min	Met One, USA		
	Corresponding Gas Analyzers	CO, SO_2, O_3	1 min	ECOTCH, Austria		
	EC/OC Analyzer	EC and OC in $PM_{2.5}$ or $PM_{1.0}$	1 h	Sunset, USA		Takegawa et al., 2009; Xiao et al., 2009
	AMS	OM and ions in $PM_{1.0}$	10 min	AeroDyne, USA		

ACPD
10, 14611–14637, 2010

Table 2. Comparison of important particle properties (mean or mean±o').

Site	$N_{20-10000}$ ($\times 10^4$ cm^{-3})	N_{Total} ($\times 10^4$ cm^{-3})	S_{Total} ($\times 10^2$ µm^2 cm^{-3})	V_{Total} (µm^3 cm^{-3})	$PM_{2.5}$ (µg m^{-3})
GZ	2.9±1.1	–	13.8±5.4	96±43	69±43
BG	1.7±0.8	1.8±0.8	9.6±4.6	94±34	69±58
Xinken	–	1.6±0.8	9.7±4.0	63±25	51±19*

* $PM_{1.8}$

ACPD
10, 14611–14637, 2010

Table 3. Increase rates of major species during the nighttime accumulation pollution episode.

Site	$N_{100-660}$ ($cm^{-3}\,h^{-1}$)	$V_{100-660}$ ($\mu m^3\,cm^{-3}\,h^{-1}$)	$M_{100-660}$ ($\mu g\,m^{-3}\,h^{-1}$)	$PM_{2.5}$ ($\mu g\,m^{-3}\,h^{-1}$)	SO_4^{2-} ($\mu g\,m^{-3}\,h^{-1}$)	NO_3^- ($\mu g\,m^{-3}\,h^{-1}$)	NH_4^+ ($\mu g\,m^{-3}\,h^{-1}$)	SNA ($\mu g\,m^{-3}\,h^{-1}$)	SNA* ($\mu g\,m^{-3}\,h^{-1}$)
BG	400	4.0	5.7	6.5	2.4	0.6	1.1	4.1	3.3
GZ	–	–	–	6.8	2.7	0.6	1.2	4.5	3.6

SNA= SO_4^{2-}, NO_3^-, NH_4^+, SNA* = $0.8\times(SO_4^{2-}+NH_4^+ +NO_3^-)$

ACPD
10, 14611–14637, 2010

Table 4. Influence of regional transport on fine particles at BG.

	$N_{100-660}$ cm^{-3}	$V_{100-660}$ $\mu m^3\,cm^{-3}$	$PM_{2.5}$ $\mu g\,m^{-3}$	$PM^{*}_{1.0}$ $\mu g\,m^{-3}$	SNA $\mu g\,m^{-3}$	SO_4^{2-} $\mu g\,m^{-3}$	NOB_3^- $\mu g\,m^{-3}$	NH_4^+ $\mu g\,m^{-3}$	OM $\mu g\,m^{-3}$
(A)	$6.2\pm2.6\times10^3$	38±16	50±29	27±13	17±10	11.8±7.1	0.9±0.8	3.8±2.2	10.9±5.0
(B)	$9.5\pm4.7\times10^3$	53±20	70±28	41±24	27±16	18.7±9.9	1.5±2.0	5.9±3.2	14.1±10.1
(B-A)/B	35%	28%	29%	33%	38%	37%	39%	35%	23%

A: Without obvious regional transport on 12 and 13 July; B: With regional transport on 19 and 21 July.
* $PM_{1.0}=SO_4^{2-}+NO_3^-+NH_4^++OM$

ACPD
10, 14611–14637, 2010

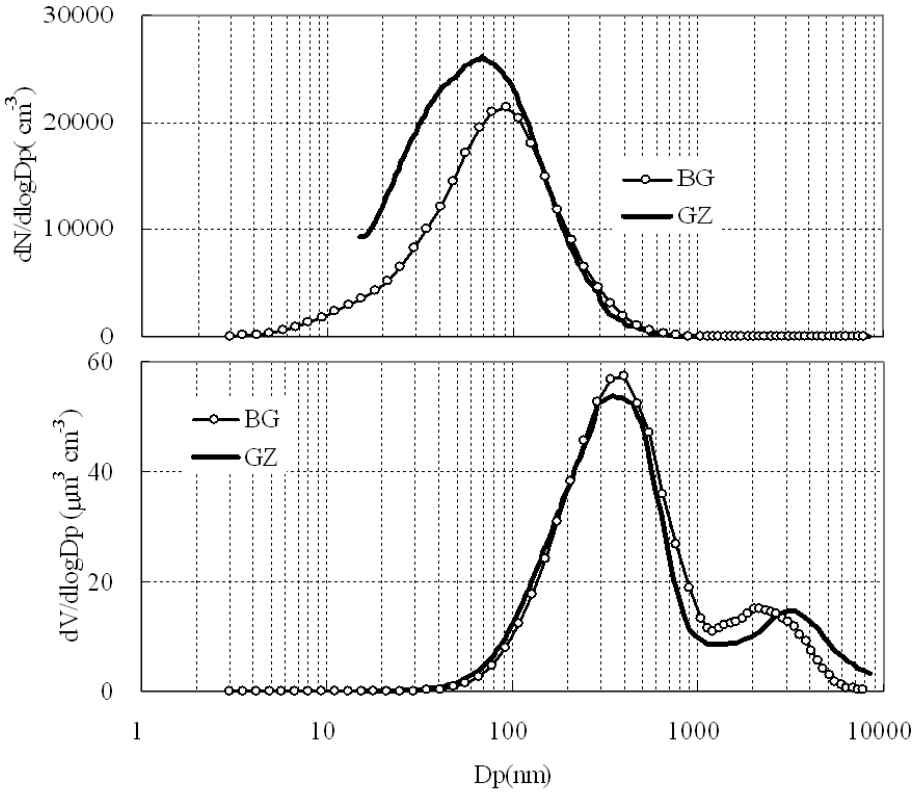

Fig. 1. Average particle number and volume size distributions at GZ and BG during the whole campaign.

ACPD
10, 14611–14637, 2010

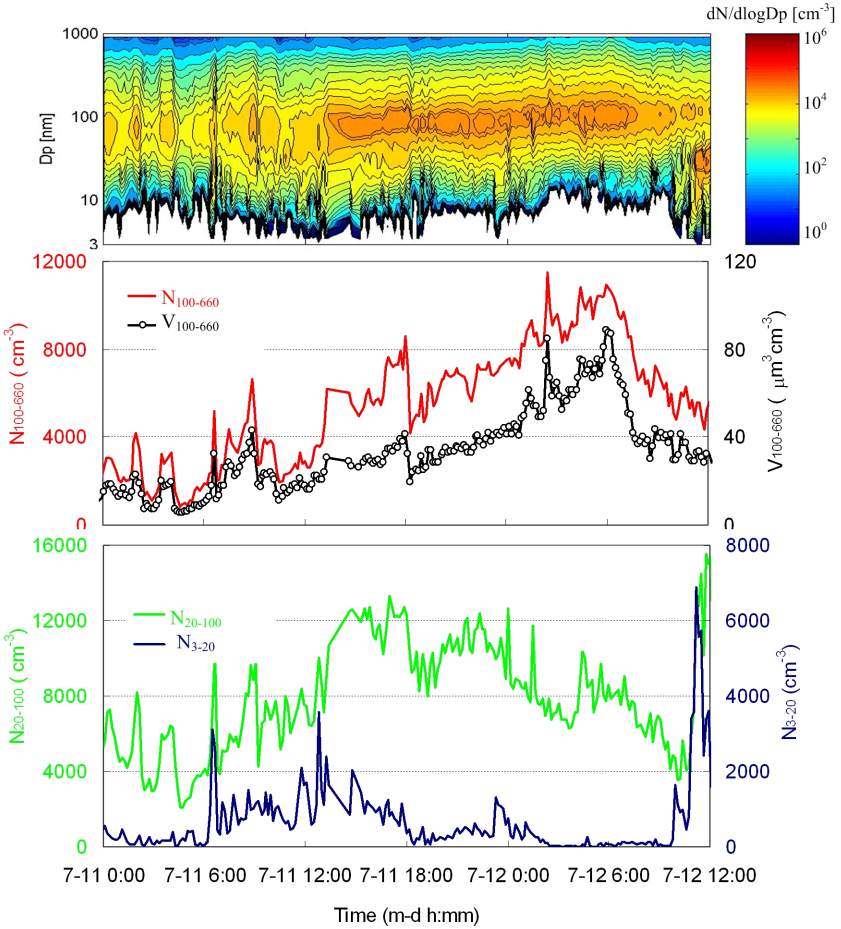

Fig. 2. Variations of particle number size distributions, number concentrations, and volume concentrations from 00:00 LT 11 July to 12:00 LT 12 July.

ACPD
10, 14611–14637, 2010

Variation of particle number size distributions and compositions

D. L. Yue et al.

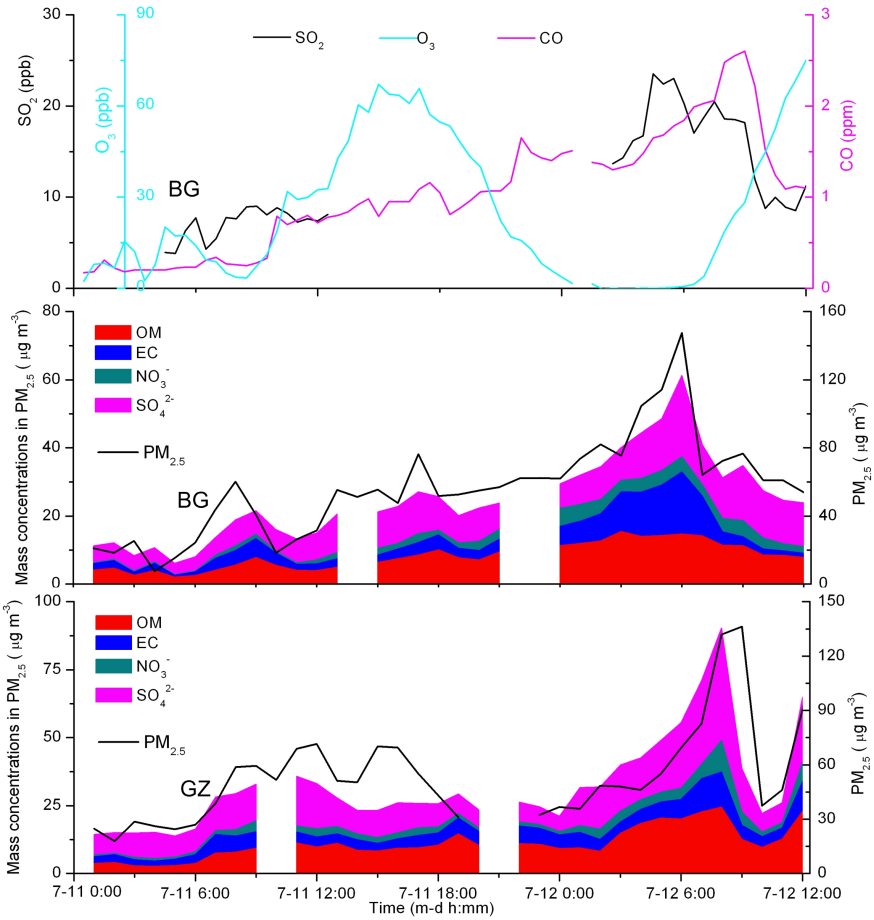

Fig. 3. Variations of trace gases at BG, $PM_{2.5}$, and mass concentrations of chemical compositions in $PM_{2.5}$ at both sites from 00:00 LT 11 July to 12:00 LT 12 July.

ACPD
10, 14611–14637, 2010

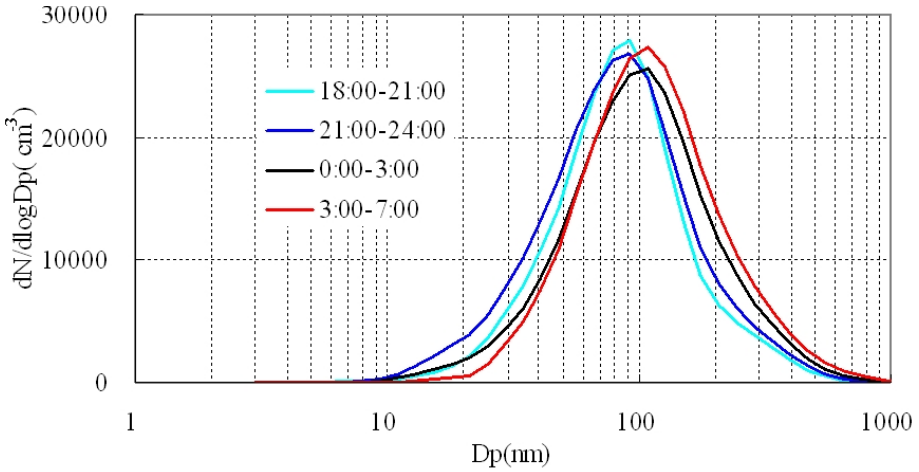

Fig. 4. Particle number size distributions during the accumulation pollution episode from 18:00 LT 11 July to 07:00 LT 12 July.

ACPD
10, 14611–14637, 2010

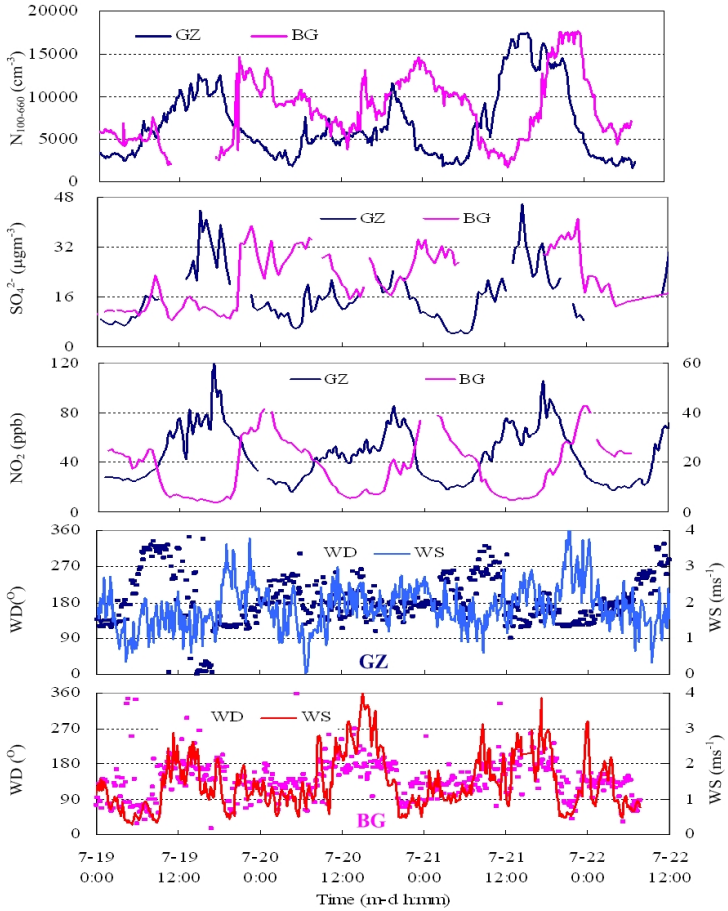

Fig. 5. Particle number concentrations from 100 to 660 nm ($N_{100-660}$), mass concentrations of SO_4^{2-}, mixing ratio of NO_2, and wind direction (WD) and wind speed (WS) from 19 to 22 July at GZ and BG.

ACPD
10, 14611–14637, 2010

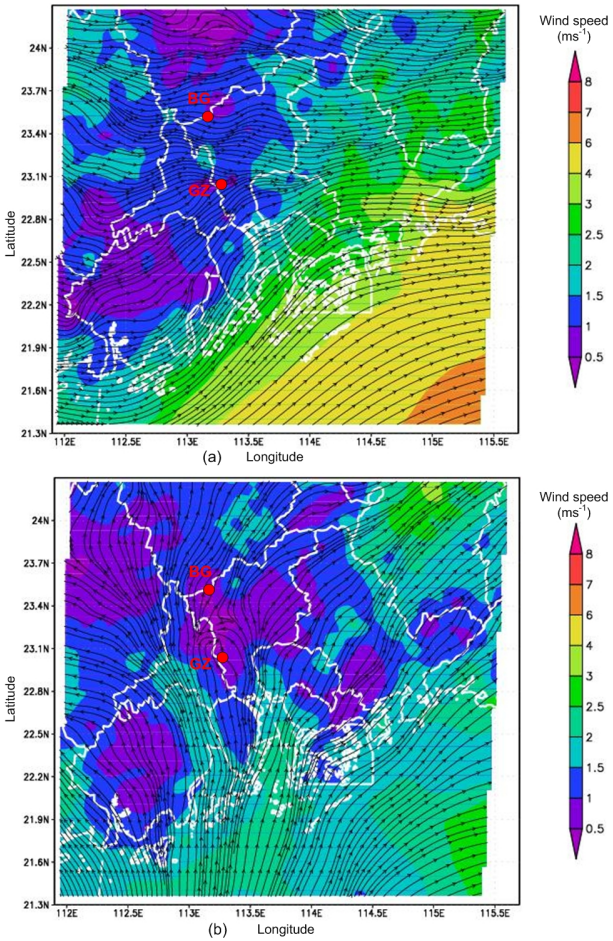

Fig. 6. Wind fields in the PRD region in the late afternoon of 12 **(a)** and 19 **(b)** July. The arrows show the directions.

ACPD
10, 14611–14637, 2010

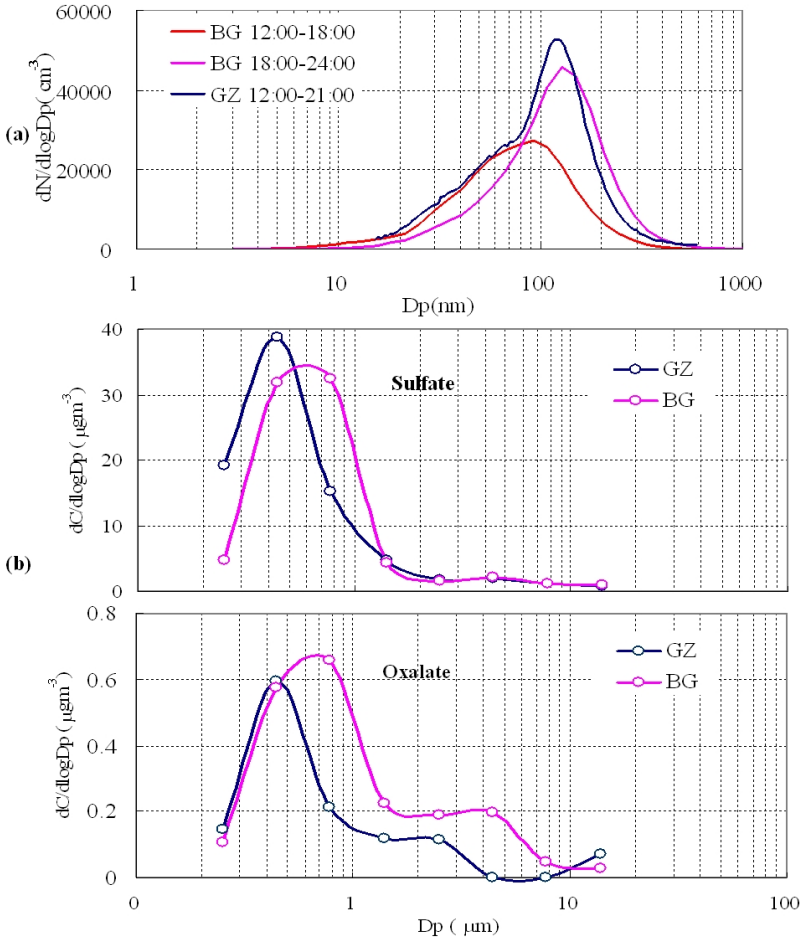

Fig. 7. Average particle number size distributions on 21 July **(a)** and average mass size distributions of sulfate and oxalate from 06:30 LT 21 July to 06:00 LT 22 July **(b)** at GZ and BG.

ACPD
10, 14611–14637, 2010